

**FuelCell2010-33329**

## **HYBRID FUEL CELL GAS TURBINE SYSTEM DESIGN AND OPTIMIZATION FOR SOFC**

**Dustin McLarty**

National Fuel Cell Research Center,  
University of California Irvine  
Irvine, CA, USA

**Prof. Scott Samuelson**

Advanced Power and Energy Program,  
University of California Irvine  
Irvine, CA, USA

**Prof. Jack Brouwer**

National Fuel Cell Research Center,  
University of California Irvine  
Irvine, CA, USA

### **ABSTRACT**

Fuel Cell–Gas Turbine (FC-GT) hybrid technology portends a significant breakthrough in electrical generation. Hybrid systems reach unprecedented high efficiencies, above 70% LHV in some instances, with little to no pollution, and great scalability. This work investigates two high temperature fuel cell types with potential for hybrid application ranging from distributed generation to central plant scales; sub MW to 100MW. A new library of dynamic model components was developed and used to conceptualize and test several hybrid cycle configurations. This paper outlines a methodology for optimal scaling of balance of plant components used in any particular hybrid system configuration to meet specified design conditions. The optimization strategy is constrained to meet component performance limitations and incorporates dynamic testing and controllability analysis. This study investigates seven different design parameters and confirms that systems requiring less cathode recirculation and producing a greater portion of the total power in the fuel cell achieve higher efficiencies. Design choices that develop operation of the fuel cell at higher voltages increase efficiency, often at the cost of lower power density and greater stack size and cost. This work finds existing SOFC technology can be integrated with existing gas turbine and steam turbine technology in a hybrid system approaching 75% fuel to electricity conversion efficiency in optimized FC-GT hybrid configurations.

### **INTRODUCTION**

The United States faces an impending energy revolution. The current means by which our transportation, residential and

industrial energy needs are met will not sustainably power our economy into the future. The evolving solution to our energy demands shifts due to rising fuel costs, environmental concerns, foreign oil dependence, and public policy. Three desirable features for future energy solutions are: diversity in primary energy sources and generation technology, improved efficiency in energy conversion and use, and optimally matching energy technologies and resources to specific uses. A new power generation technology that should represent a portion of any diverse energy portfolio is fuel cell-gas turbine hybrid, FC-GT, technology. FC-GT technology significantly improves power generation efficiency, and can use a variety of light hydrocarbon fuels [1].

Integration of fuel cell and gas turbine technologies into a single symbiotic system represents a breakthrough in electricity production technology. Gas turbine performance limitations result from the Carnot Limit and the entropy generated through combustion of fuel. Conversion of fuel to heat reduces the potential for useful work, and the Carnot principle limits the subsequent conversion of heat into mechanical energy. A fuel cell extracts work directly from the available Gibbs free energy. However, a fuel cell cannot produce power while fully utilizing the fuel and the wasted fuel hampers efficiency. A delicate balance of power and efficiency ensues without the implementation of a means to fully utilize the fuel in the anode off-gas. Hybrid FC-GT systems can effectively use fuel cell heat and anode off-gas fuel to produce electricity and compressor power.

Molten carbonate and solid oxide fuel cells are two fuel cells types that are well-suited for hybridization with a gas

**Nomenclature**

A	Area
C	Thermal Capacitance
$c_p$	Constant Pressure Specific Heat
$c_v$	Constant Volume Specific Heat
Flow	Turbomachinery Flow Rate
h	Enthalpy
$h_c$	Convection Coefficient
$k_c$	Conduction Coefficient
m	Mass
M	Mach Number
N	Normalized Turbomachinery Parameter
$\dot{n}$	Flow Rate
P	Pressure
PR	Pressure Ratio
Q	Sensible Enthalpy of Transfer Ions
RPM	Shaft Speed
$R_u$	Universal Gas Constant
T	Temperature
V	Velocity
$\dot{W}$	Power
$\nabla$	Volume

**Greek Letters**

$\gamma$	Specific Heat Ratio
$\varepsilon$	Emissivity
$\eta$	Efficiency
$\rho$	Density
$\sigma$	Boltzmann Constant
$\chi$	Concentration

**Subscripts**

0	Stagnation
B	Blower
cyc	Cycle
des	Design
FC	Fuel Cell
fuel	Fuel
Gen	Generator
HXnode	Heat Exchanger Node
in	Inlet
isen	Isentropic
net	Net power
out	Outlet
re	Re-circulated Gas Stream
s	Solid
turb	Turbine

turbine generator [2]. Both types operate at high temperatures, and thus produce high quality heat that is ideal for producing additional power in a turbine. These fuel cell hybrids have a range of applications from the distributed generation, sub-megawatt, and scale to large central power plants producing hundreds of megawatts to gigawatts.

Accurate simulation of FC-GT behavior can be achieved only by a methodology meeting the following guidelines.

- Physical and chemical behaviors of each component must be resolved from first principles with the exception of

compressor and turbine components with well defined empirical maps. The fuel cell must calculate Nernst potential and loss parameters from governing equations of electrochemistry and can not be based on a single V-I curve. The V-I curve methodology is insufficient to capture the changes when temperature, oxidant concentration, or fuel utilization changes [3].

- Dimensional models are superior to bulk models for their ability to capture detailed spatial information and accurate temperature and concentration profiles. Bulk models are computationally efficient and useful for first approximations, but only estimate average heat transfer. Nodal fuel cell models capture local conditions for accurate calculation of Nernst potential and loss terms.
- Careful consideration must be taken when approximating the heat transfer between nodes, as certain assumptions can have a large impact on temperature profiles and performance in a nodal model. Physical parameters including wall thickness and channel dimensions are critical in determining the convective and conductive surface areas between nodes. The principle means of heat mobility throughout the stack is conduction through the solid materials and must be determined as accurately as possible. Material properties specifications are important to approximate conduction as more conductive materials move heat quicker and reduce thermal gradients.

Simulating a specific FC-GT hybrid for a design study, and simulating a generic FC-GT hybrid for dynamics and control studies require different parameter specifications. Designing a scalable model that is based on the use of several dimensionless parameters leads to robustness and versatility. Determining the turbomachinery size to meet requirements at optimal fuel cell conditions is a great starting point for sizing all balance of plant components and selecting the hybrid system operating point. SOFC stacks are characterized by several key parameters, notably average operating temperature, operating pressure, operating power density, fuel utilization, and maximum temperature rise across cell. This sufficiently constrains the balance of plant design; however, with the addition of cathode recirculation and bypass flows additional parameters can be varied to achieve optimal performance under a range of conditions.

The current study developed the following methodology for sizing the balance of plant components.

1. Simulate the fuel cell and determine the inlet, outlet temperatures that satisfy temperature constraints over a range of operating conditions.

2. Simulate the balance of plant components with steady state fuel cell outlet conditions and iteratively approach the fuel cell inlet conditions.
3. Adjust the mass flow of the turbomachinery and size of the heat exchangers to match the inlet conditions of the fuel cell while operating turbomachinery at design RPM and pressure ratio.
4. Combine the dynamic fuel cell and dynamic balance of plant components into a single model with the sizing and operating conditions specified by their respective individual models.

This repeatable methodology can be used for a parametric variation hybrid FC-GT system design study. The parametric study in this work yielded valuable insights regarding design parameters that should be considered when developing these types of hybrid systems. Figure 1 details the process of optimizing each hybrid configuration for a specific set of design parameters. Three models were used to converge to an optimal configuration.

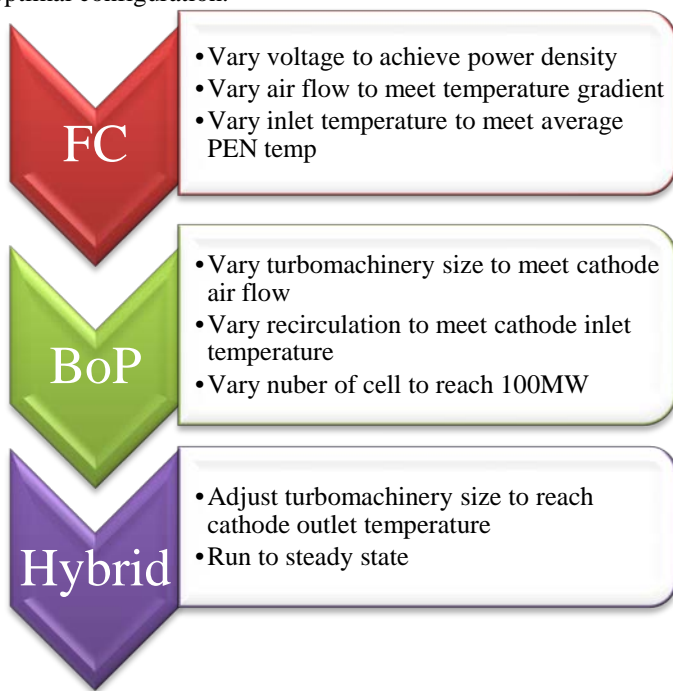


Figure 1 Hybrid Design Methodology

The parameters used to specify the design point of a fuel cell are average operating temperature, operating power density and voltage, and temperature rise across a single cell. The values are shown in Table 1.

The turbomachinery model offers a high degree of adjustability and can utilize 10 different compressor and turbine maps to easily matching performance of any specific turbine. The system utilizes generic performance maps or imports specific manufacturer data for calculating mass flow rate and efficiency at any shaft speed, pressure ratio, and inlet

temperature. The generic empirical maps studied are sufficient to accommodate radial or axial, single or multi-spool turbine designs. An example of a single spool, axial, compressor and turbine map operating near its design point are shown in Figure 2

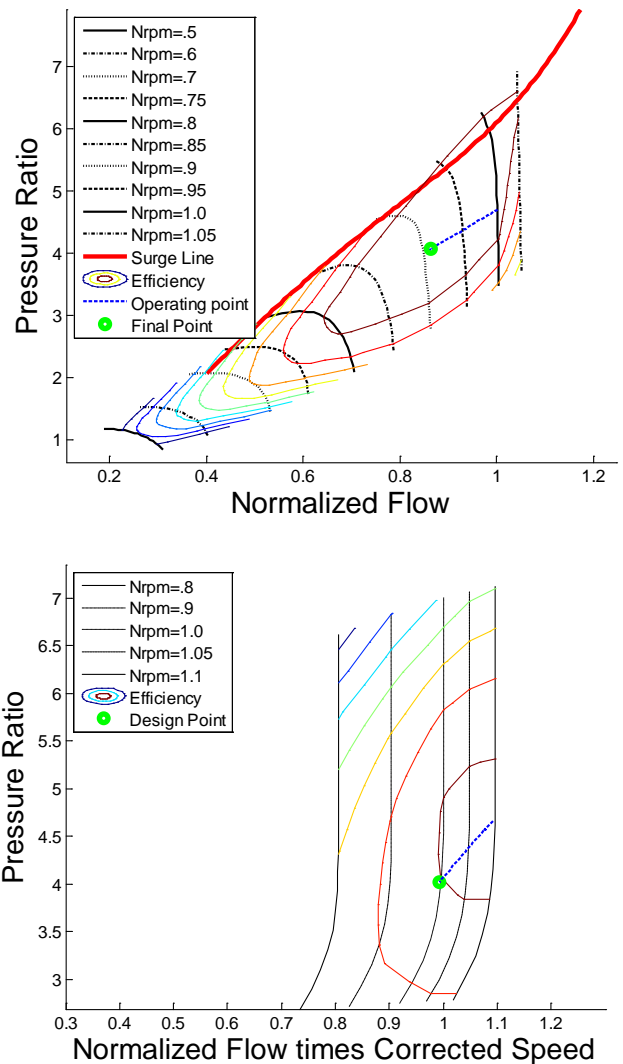


Figure 2. Empirical Compressor and Turbine Maps

Table 1. Fuel Cell Operating Requirements

Fuel Cell Type	SOFC
Operating Power Density	100-700 (mW/cm <sup>2</sup> )
Average Operating Temperature	700-850°C
Limiting Stack Temperature Rise	50-100°C

## BACKGROUND

### *Molten Carbonate and Solid Oxide Fuel Cell Hybrids*

Reformation of methane-containing fuels using high temperature steam comprises an integral part of modeling both molten carbonate and solid oxide Fuel Cells. Reformation kinetics for steam reformation of methane accompanied by water-gas shift is the principle means for hydrogen or synthesis gas production [4]. Experimental results from Xu and Froment's work determined a single set of three global rate expressions that describe the kinetic processes between 675-1000°K. This temperature range satisfies the conditions in the reforming and anode channels of the fuel cells of this study.

The integration of a fuel cell and gas turbine presents several operational synergistic effects. Most notably the gas turbine is driven off the waste heat of the fuel cell, and the air flow to the fuel cell is provided by the air movement of the gas turbine rather than the parasitic load of an air blower. Varying the cell size and the fuel utilization in the cell can help optimize the integration [5]. Independent operation of FC systems may differ in fuel utilization from the optimal hybrid configuration. Lower fuel utilizations reduce the losses in the fuel cell, and the unspent fuel can be burned and provide thermal energy for the turbine in a hybrid configuration.

Work on the dynamics of an integrated FC-GT hybrid system has been ongoing at the NFCRC for more than ten years. Early work in collaboration with the NETL in determined that to allow for large turndown capabilities, creative control strategies would be required to protect sensitive equipment during perturbations [6]. This initial work included carbonate fuel cell models previously validated on the ability to simulate internal reformation of methane. Each laboratory independently developed individual models using different software packages. Identical assumptions were made for each component, but slight differences existed in the solution strategy and compressor maps used.

The steady state results compared favorably, yet dynamic responses differed with alternative control strategies. The NFCRC control strategy maintained oxidizer temperature with fuel flow rate; impacting fuel utilization yet providing fixed inlet conditions for the gas turbine. The NETL strategy maintained constant fuel utilization and fixed oxidizer temperature by controlling airflow. Both strategies aimed to maintain constant cathode inlet temperature and minimize fuel cell temperature transients.

More recent work added the capability of simulating a variable speed compressor. This allowed for an additional control input for maintaining cathode inlet temperature that both lab models showed decreasing in the previous work [7] [8]. The results presented in this study showed improvements in the controllability of the stack temperature. Again it was noted that the load shed resulted in a lower fuel cell power, lower GT power, and slightly higher efficiency.

Fuel cells provide excellent performance when considering conversion efficiency or emissions, but current systems are expensive without subsidies. The market penetration of this technology is currently limited by high capital cost. Natural gas

pipeline pressure reduction stations present one possible market for high temperature fuel cell systems that may become very attractive as capital costs come down [11]. The work of Rashidi et al. models an existing gas pressure reduction installation from Enbridge in Toronto, Canada, with a detailed thermodynamic analysis and lifetime cost analysis. The natural gas pipeline operates at 350 psi, and must pass through a turbo-expander to reduce the pressure for household consumption. The turbo-expander produces 1MW of electricity, but, without heating, would reduce the temperature to below freezing.

The installed MCFC cogeneration plant replaces a previous system that employed a natural gas fed burner to supply the necessary heat in the Rashidi et al. study. In the new system natural gas from the low pressure stream is fed into a 1.2 MW MCFC that produces electricity and waste heat that pre-heats the high pressure gas stream before it is expanded. The entire system is designed to produce 2.2MW of electricity and 6000 m<sup>3</sup>/hr of low pressure natural gas. The cost analysis includes all overhead costs, material and labor costs, and a 4% annual cost increase. The payback period of the system is heavily dependent on future electricity and natural gas costs. Several different future cost scenarios were considered including some that account for a carbon offsetting value that may be implemented by future governments. The lifetime amortization is significantly reduced by any form of carbon offset value. With electricity rates as high as those in Germany the system pays for itself in only five years.

Most SOFC-GT hybrid systems demonstrated to-date have operated in a very narrow range suited to maintain steady fuel cell temperature and minimize degradation. Burbank et al. introduce two additional degrees of control by utilizing a variable-geometry nozzle turbine, and an auxiliary combustor that can provide additional heat to the turbine inlet stream. This new system configuration allows for a system wide turndown ratio of 5:1, meaning the system can safely operate at 20% power production capacity [12]. No bypass or bleed flow paths were needed to accomplish this turndown. The system performs best, 63% efficient, at 30% power and operates at 53% efficiency at full power.

The work of Jaroslaw et al. characterizes off-design performance of hybrid systems by simulating a pre-commercial tubular SOFC stack from Siemens-Westinghouse Power Corporation using a zero-dimensional approach to determine the possibility of operation for a set of specific design parameters. The analysis determined thousands of valid operating points, plotted into maps characterizing the system at off-load performance [13].

The world's first pressurized SOFC-GT hybrid prototype was tested at the University of California, Irvine. A Siemens-Westinghouse tubular fuel cell stack producing 180kWe, and was paired with a 75kW Ingersoll-Rand gas turbine to produce up to 220kW during 2900 hours of testing at the NFCRC. The data gathered validated modeling approaches developed at the NFCRC [14]. The system achieved fuel to electric efficiencies of 53%. The use of FC-GT hybrids is not limited solely to terrestrial power generation applications. Interest has arisen



computing cost. The design of this model applies to generic or specific fuel cells including the DFC line from FCE and adjusts to represent any planar type MCFC or SOFC. The details of this HT-FC model are presented in reference [18].

### Compressor/Turbine

A simple steady-state Brayton cycle analysis does not lend itself to dynamic modeling of real gas turbine systems, when only inlet conditions are known. The dynamic compressor and turbine models employed in this work make efficient use of a variety of steady-state performance maps. The overall approach solves a dynamic shaft speed equation based upon a torque balance and dynamic equations that allow mass storage in diffuser volumes downstream from the compressor and turbine. The compressor and turbine performance characteristics that feed into these dynamic equations are determined by movement within steady-state performance and efficiency maps. The configuration and input-output structure of the 2-D maps are shown in Figure 4. Shaft speed, pressure ratio, and flow rate are normalized using the following equations.

$$N_{RPM} = RPM \sqrt{T_0/T_{des}} \cdot RPM_{des} \quad (1)$$

$$N_{Flow} = \frac{Flow}{Flow_{des}} \cdot \frac{\sqrt{T_0/T_{des}}}{P_{in}/P_{des}} \quad (2)$$

$$PR = \frac{P_{out} \cdot P_{des}}{P_{in} \cdot PR_{des}} \quad (3)$$

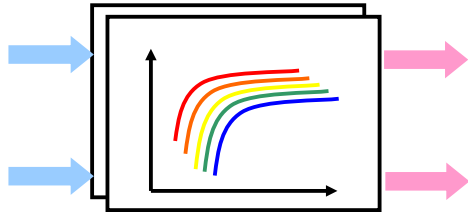


Figure 4. Empirical Map Flow Diagram

Where:

$$\text{Stagnation temperature} \quad T_0 = T_{in} \cdot \left( 1 + M^2 \left( \frac{\gamma - 1}{2} \right) \right) \quad (4)$$

$$\text{Mach Number} \quad M^2 = \frac{R_u \gamma T_{in}}{MV_{in}^2} \quad (5)$$

$$\text{Velocity} \quad V_{in} = \frac{\dot{n} R_u T_{in}}{A_{in} P_{in}} \quad (6)$$

$$\text{Specific Gas Constant} \quad \gamma = \frac{c_p}{c_v} = \frac{c_p}{c_p - R_u} \quad (7)$$

Despite similarities the compressor and turbine models must employ different solution strategies. The input parameters for the compressor model are ambient temperature, and species concentration, shaft speed, as well as the inlet and outlet

pressures. The inlet pressure is ambient air pressure, and the outlet pressure is found by backwards solving the pressure loss through each hybrid system component from the known exhaust pressure. Conservation of energy applies to both the gas stream and solid material of the compressor. The following equations detail the results of the control volume analysis with the subscripts *s*, *f*, *a* representing the solid, fluid, and ambient conditions, and  $h_c$  is an approximate convective heat transfer parameter.

$$\frac{dT_f}{dt} = \frac{\dot{W} + (h\dot{n})_{in-out} + h_c A (T_s - T_f)}{c_p \frac{P_{out} \nabla}{R_u T_{flow}}} \quad (8)$$

$$\frac{dT_s}{dt} = \frac{h_c A (T_f - T_s) + \epsilon \sigma A (T_a^4 - T_s^4)}{c_p m} \quad (9)$$

Where all sensible enthalpies,  $h$ , are calculated using temperature curve fits and isentropic efficiency determined by the look-up table:

$$\dot{W} = \dot{n}_{out} \left( \frac{h_{isen} - h_{in}}{\eta_{isen}} \right) \quad (10)$$

$$T_{isen} = (PR \cdot PR_{des})^{\gamma-1/\gamma} \quad (11)$$

The turbine performance is solved knowing the inlet temperature, outlet pressure, flow rate, and species concentrations. Again, a back calculation of the downstream components determines turbine outlet pressure. This information solves for turbine inlet pressure, outlet temperature, and shaft power produced. Due to the format of the normalized flow tables the system model requires an iterative approach to finding the inlet pressure. The inlet pressure determines pressure ratio, which fixes the mass flow rate when applied to the turbine map tables. The mass flow exiting the turbine must converge with the incoming flow to conserve mass.

A looped integral approach determines flow rates in all components downstream of the compressor; known hereafter as a plenum volume calculation. In all other components the pressure integral will be paired with an equation for mass flow rate based on laminar flow with a friction factor derived from the Darcy friction equation. Again, conservation of energy applied to the turbine air stream and solid components is performed in addition to the turbine map calculations, which follow the same process as the compressor maps, and the plenum volume calculation expressed below. In these equations the subscripts *s*, *f*, and *a* specify the solid, fluid, and ambient conditions.

$$\frac{dP}{dt} = \frac{(\dot{n}_{in} - \dot{n}_{out}) \cdot R_u \cdot T_{flow out}}{\nabla_{turb}} \quad (12)$$

The conservation of energy for the turbine air flow and solid material are as follows:

$$\frac{dT_f}{dt} = \frac{\dot{W}_T + (h\dot{n})_{in-out} + h_c A (T_s - T_f)}{c \frac{P_{out} \nabla_{turb}}{R_u T_{out}}} \quad (13)$$

$$\frac{dT_s}{dt} = \frac{h_c A (T_f - T_s) + \epsilon \sigma A (T_a^4 + T_s^4)}{c_p m} \quad (14)$$

The slightly different equation for shaft power and isentropic temperature of the turbine flow are presented below where  $\eta_T$  represents the turbine efficiency found from the generic map:

$$\dot{W}_T = (h\dot{n})_{in} - \dot{n}_{out}[h_{in} - (h_{in} - h_{ises})\eta_T] \quad (15)$$

$$T_{isen} = \left( \frac{1}{PR \cdot PR_{des}} \right)^{\gamma-1/\gamma} \quad (16)$$

Axial and radial turbomachinery operates on a single shaft to eliminate gears and unnecessary transfer losses between the turbine and compressor. However, a single shaft limits the compressor and turbine to operation at the same real shaft speed. Electric generators are classified as either synchronous, operating at 60 Hz (50 Hz in Europe), or asynchronous, requiring power conditioning devices to prepare the electricity for grid distribution. This study uses a dynamic shaft model for simulation of asynchronous plants, however, the scope of this design analysis is limited to steady performance, and thus explanations of the rotational inertia calculations will be omitted here.

#### Heat Exchangers

Hybrid FC-GT systems often require high temperature heat exchangers, most commonly manufactured from stainless steel and/or ceramics in a planar configuration.

The current heat exchanger model uses ten control volumes, nodes, evenly spaced along the length of the fluid channels to yield a spatial temperature profile and avoid the pinch-point limitations of a bulk heat exchanger model. The surface area of the heat exchanger can be adjusted by varying the number of plates, rather than changing the planar dimensions of each plate. This modeling technique gives an approximation of the surface area required to meet the particular design needs with low computational cost. The following energy balance equations are applied to each control volume.

$$\frac{dT_{hot}}{dt} = \frac{(h\dot{n})_{in-out} - h_c A \left( \frac{T_{in} + T_{out}}{2} - T_s \right)}{c_v \cdot \nabla_{HXnode} \cdot C} \quad (17)$$

$$\frac{dT_{cold}}{dt} = \frac{(h\dot{n})_{in-out} - h_c A \left( \frac{T_{in} + T_{out}}{2} - T_s \right)}{c_v \cdot \nabla_{HXnode} \cdot C} \quad (18)$$

$$\frac{dT_s}{dt} = \frac{\begin{bmatrix} h_c A \left( \frac{T_{in} + T_{out}}{2} \right)_{cold} - T_s \\ h_c A \left( \frac{T_{in} + T_{out}}{2} \right)_{hot} - T_s \end{bmatrix}}{k_c A (T_{n+1} + T_{n-1} - 2 \cdot T_s) / L_{node}} \quad (19)$$

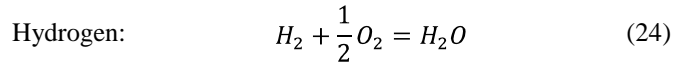
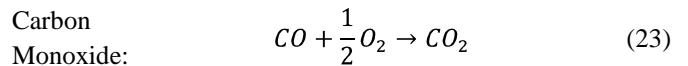
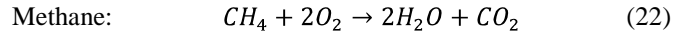
#### Oxidizer/Combustor

An oxidizer or combustor combines the anode off gas and some of or the entire cathode stream to react the remaining fuel unused by the fuel cell. The oxidizer can also be fired with additional fuel. The oxidizer converts the remaining chemical energy of the fuel to heat, and reduces the concentration of fuel constituents. A hybrid FC-GT design uses this heat to drive the turbine, powering the compressor and producing additional electricity. The oxidizer modeled in this work accounts for three inlet streams; anode exhaust gas stream, fresh fuel stream, and pre-heated air stream. Some designs supply fuel directly to the combustor as a means of increasing turbine inlet temperature, controlling the system, and/or dynamically increasing system output; however, this reduces system efficiency and should be limited to start-up and shut-down procedures if high efficiency is paramount. Anode off-gas has little heating value, and carries significant water and carbon dioxide, thus it burns quite cool. When mixing these three streams conservation of mass and continuity are applied to find the molar flow rate and mixed species concentrations. The following two expressions are used to find the composition of the mixed gas stream pre-combustion.

$$\dot{n}_{out} = \sum (+(\dot{n}X_i)_{fuel} + (\dot{n}X_i)_{off}) \quad (20)$$

$$x_{out,i} = \frac{(\dot{n}X_i)_{air} + (\dot{n}X_i)_{fuel} + (\dot{n}X_i)_{off}}{\dot{n}_{out}} \quad (21)$$

The combustion modeled in this work accounts for the same seven species as the remainder of the model, and does not consider reaction kinetics. The effects of equilibrium states and incomplete combustion are lumped into a single reaction effectiveness term for each of the three reactions considered. The three reactions considered in this combustor model are shown below.



Once again a control volume conservation of energy approach is employed to balance the energy flowing into the combustor, the energy flowing out of the combustor, the heat lost to the environment, and the heat generated by the combustion process.

$$\frac{dT_c}{dt} = \frac{\begin{bmatrix} h_c \cdot A \cdot (T_c - T_{amb}) + (h\dot{n})_{air} \\ + (h\dot{n})_{off} + (h\dot{n})_{fuel} \\ - (h\dot{n})_{out} - Q_{ion\ transfer} \end{bmatrix}}{C_p \frac{P_{comb} \nabla_{comb}}{R_U T_{comb}}} \quad (25)$$

### Mixing Chamber

Both MCFC and SOFC hybrid systems utilize some form of recirculation and or bypass, and the mixing of the primary and re-circulated streams must be modeled. In this work a simple bulk mixing model is employed, and like all other components it is assumed to be perfectly stirred and non-reacting. Continuity and conservation of mass account for the flow rate of each species and determines the composition of the flow exiting the mixing chamber. Conservation of energy determines the exit temperature of the mixed gas and accounts for ambient losses with a separate energy balance for the mixing chamber.

$$\dot{n}_{mix} = \sum ((\dot{n}X_i)_1 + (\dot{n}X_i)_2) \quad (26)$$

$$X_{mix,i} = \frac{(\dot{n}X_i)_1 + (\dot{n}X_i)_2}{\dot{n}_{mix}} \quad (27)$$

$$\frac{dT_{mix}}{dt} = \frac{\left[ h_c \cdot A \cdot (T_{mix} - T_{pipe}) + (h\dot{n})_1 + (h\dot{n})_2 - (h\dot{n})_{mix} \right]}{c_p \frac{P_{mixer} \nabla_{mixer}}{R_U T_{mix}}} \quad (28)$$

### Blower

A blower operates similar to a compressor, but with a much lower pressure ratio. This analysis treats the blower as a compressor with fixed isentropic efficiency, and calculates power requirements for generating sufficient pressure rise. The recirculation of cathode exhaust is performed by applying a control volume energy conservation analysis accounting for energy lost to inefficiencies and cooling. A second energy conservation analysis accounts for the temperature of the blower and the heat radiated to the ambient conditions. Here the subscript *re* defines the re-circulated gas stream and once again *s* and *a* represent the solid and ambient conditions.

$$\frac{dT_{re}}{dt} = \frac{\dot{W}_B + (h\dot{n})_{in-out} + h_c A (T_s - T_{re})}{c_p \frac{P_{out} \nabla}{R_U T_{re}}} \quad (29)$$

$$\frac{dT_s}{dt} = \frac{h_c A (T_{re} - T_s) + \epsilon \sigma A (T_a^4 - T_s^4)}{c_p m} \quad (30)$$

Where the blower power is calculated using the following energy balance wherein the sensible enthalpy under isentropic conditions,  $h_{isen}$ , is found as a function of the isentropic temperature described in (32).

$$\dot{W}_B = \dot{n}_{out} \left( \frac{h_{isen} - h_{in}}{\eta_{isen}} \right) \quad (31)$$

$$T_{isen} = \left( \frac{P_{out}}{P_{in}} \right)^{\gamma-1/\gamma} \quad (32)$$

### Net Power and Efficiency

Power generation comes from three different sources in the FC-GT hybrid system, and all three must be accounted for when calculating the net power and efficiency of the system. The system efficiency is found using known heating values for the fuel, multiplying by the fuel flow rates, and dividing this into the net power produced. This can be performed using the expressions below with the fuel heating values presented in Table 2.

$$\dot{W}_{Net} = \dot{W}_{Turb} + \dot{W}_{FC} + \dot{W}_{Gen} \quad (33)$$

$$\eta_{cyc} = \frac{\dot{W}_{Gen}}{\dot{n}_{fuel} HV_{fuel}} \quad (34)$$

**Table 2. Fuel Heating Values**

Fuel	Lower Heating Value	Higher Heating Value
	(LHV)	(HHV)
	(kJ/kmol)	(kJ/kmol)
CH <sub>4</sub>	802952.15	890835.7
H <sub>2</sub>	240424	284469.4
CO	305200	305200

### STEADY STATE DESIGN PERFORMANCE RESULTS

Seven different parameters are investigated for their impact on performance and cost. These seven parameters are listed below.

1. Temperature differences across the fuel cell stack
2. Fuel cell operating power density
3. Fuel cell fuel utilization
4. Air pre-heating
5. Peak turbine efficiency
6. System operating pressure
7. Fuel cell PEN average operating temperature

This section presents results for the SOFC hybrid system of Figure 2. Table 3 presents a comparison for the system values for the specific cases of 80% fuel utilization, 200°C gain across the stack, a power density of 500mW/cm<sup>2</sup>, with different amounts of air pre-heating. The subsequent figures have all been normalized to the parameters for the base cases presented in Table 3.

**Table 3. Initial Design Results**

System Parameter	Units	0°C Air Pre-Heat	100°C Air Pre-Heat	200°C Air Pre-Heat
Voltage	Volts	0.855	0.863	0.866
ΔT PEN	°K	101.7	100.4	96.8
Stack Size	Cells	306,400	303,700	302,200
Stack Power	MW	84.1	83.5	83.4
Gen Power	MW	16.6	17.1	17.0
Blower Power	MW	.70	.55	.40

<b>Efficiency</b>	%	65.0	66.1	66.4
<b>Comp Size</b>	Kg/s	74.4	87.7	107.2
<b>Turbine %</b>	%	16.5	17.0	17.0
<b>Air Heater</b>	plates	0	891	2762
<b>Fuel Heater</b>	plates	1042	1898	2270
<b>Turbine Inlet</b>	°K	1332	1220	1095
<b>Recirculation</b>	%	64.09	55.54	42.28
<b>Peak Temp</b>	°K	1072	1072	1071
<b>Cath Outlet</b>	°K	1061	1061	1061

### 1. Stack Temperature Rise

This study first investigated the impact of stack temperature gradient on performance. Expectations were that greater temperature rise across the stack requires less air flow, and thus smaller turbomachinery, resulting in higher system efficiency. The model supported this prediction, but to a lesser extent than was expected. Figure 5 presents the normalized results of this sensitivity analysis. Reducing the temperature differential 50°C decreased the overall system efficiency by only 0.3%. This lower than anticipated reduction in efficiency is likely due to the use of a gas turbine instead of separate power for the air compressor. Reductions in stack temperature differential significantly decrease the PEN temperature gradient. The trend toward lower efficiency with less stack temperature rise can be explained by the combined effect of several shifts. To maintain the same average PEN temperature, the inlet air must be heated to a higher temperature, thus the greater recirculation. The increased recirculation not only requires a greater amount of power to be consumed in the blower, but decreases the average oxygen concentration in the cathode, and thus decreases the cell voltage as well. The additional air used to reduce the stack temperature gain reduces the combustor temperature and the exhaust temperature, thus requiring a much larger heat exchanger to pre-heat the incoming fuel. The larger turbomachinery does produce a greater portion of the net power, but comes with a small penalty in overall efficiency.

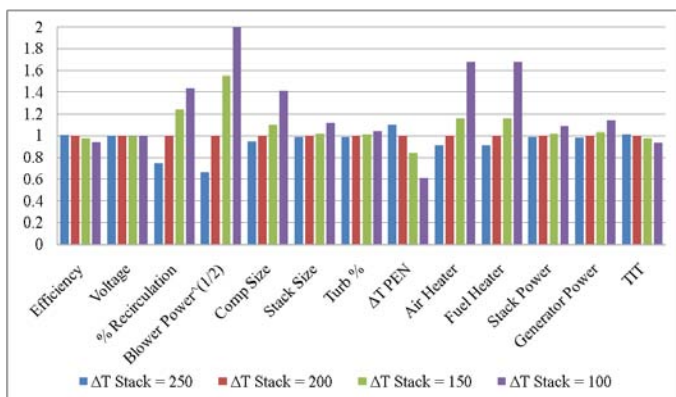
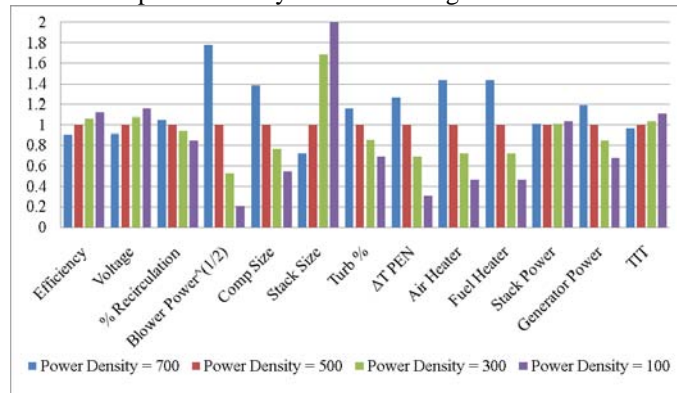


**Figure 5. Design Impact of Stack Temperature Profile**

### 2. Fuel Cell Operational Power Density

The second operating condition studied was fuel cell power density. Variations in operating power density present a clear

trade-off between cost and efficiency. Fuel cells operate closest to their ideal efficiency at extremely low power densities, but achieving more power from the same size stack is possible if only slightly less efficient. Stand alone fuel cell systems will exhibit efficiency behavior closely mirroring the polarization curve. A hybrid system, however, has the luxury of capturing a portion of the fuel cell generated heat, thereby reducing the negative impact of operating at higher power densities. Thus it can be shown that the ideal power density for a fuel cell operated in a hybrid system is greater than that of the same fuel cell operated in a stand-alone system. The impact of reducing the fuel cell power density is shown in Figure 6.



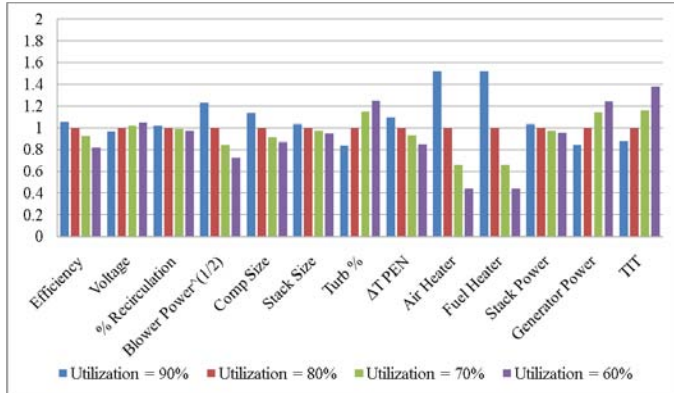
**Figure 6. Design Impact of Stack Power Density**

Figure 6 confirms lower operating power densities result in higher efficiencies. The operating voltage sees a greater differential drop with increasing power density than the system efficiency due to the hybrid ability to recapture fuel cell heat. Reducing power density from 600 mW/cm<sup>2</sup> to 200 mW/cm<sup>2</sup> increased efficiency from 63% to 70% LHV, yet requires a threefold increase in stack size to achieve the same system power. This trend indicates that a properly designed hybrid system should achieve higher efficiencies when operating below design power. This is contrary to most electrical generating technologies that can often exhibit steep performance drop offs when operating below design output.

Figure 6 results show an inverse relationship between voltage and compressor size, and between voltage and PEN temperature gradient. Fixed recirculation implies the changing compressor size entirely accounts for the reduced air flow rate. This makes physical sense in that recirculation controls the inlet temperature by mixing a specific ratio of compressor air with cathode exhaust. Fixed recirculation indicates a minimal change in compressor and cathode exhaust temperatures. The sharp drop off in blower power requirements indicates a much smaller pressure differential between cathode inlet and outlet. This corroborates well with the drop in required cathode air flow, as pressure loss increases with velocity squared. Interestingly, the TIT rises at lower power density. The same amount of anode off-gas oxidizes with less air flow producing higher temperatures (and lower mass flow) entering the turbine.

### 3. Fuel Cell Operational Fuel Utilization

The next operating condition investigated was fuel utilization. Other authors have hypothesized that operating below optimal fuel efficiency in the fuel cell would increase the turbine inlet temperature, and produce more energy from the turbomachinery. Despite the fact that the fuel is underutilized in the more efficient of the two devices, the fuel cell, these authors argue that the benefits to the stack voltage and TIT outweigh the additional fuel.



**Figure 7. Design Impact of Stack Fuel Utilization**

The results presented in Figure 7 show a steep decline in system performance, from 65% to 52% LHV, with decreasing fuel utilization. This system decline occurs despite the rise in fuel cell operating voltage and TIT, as others have predicted. Operating this hybrid cycle at reduced fuel utilizations does provide some interesting side benefits. The stack size is reduced due to the greater amount of power derived from the generator, the compressor size and PEN temperature gradient are reduced due to the higher operating voltage, the parasitic blower power is reduced due to the reduction in cathode air flow, and the fuel heater size is reduced due to the higher TIT at which heat is exchanged.

### 4. Air Pre-Heat

A thermodynamic cycle that recuperates more heat typically performs more efficiently. Advanced Brayton cycles achieve recuperation through inter-cooling and staged compression through the use of large and efficient heat exchangers. Applying a heat exchanger of this type to the SOFC-GT hybrid allows post-combustor gases to pre-heat the incoming air. This reduces the cathode recirculation required, and can likewise improve system efficiency. The results showed the benefits of heat recuperation are minimal at best when applied at this point in the cycle, which is expected due to the entropy generation associated with heat exchange at high temperature differential. Figure 7 indicates an improvement from 65% to 66% LHV with 200°C of pre-heating, but a net loss of power when a steam bottoming cycle is applied. Reduced recirculation increases necessary turbomachinery size, while lower turbine inlet temperature reduces efficiency. These combined changes yield similar power production from the turbomachinery.

Figure 8 would seem to indicate the inclusion of an air pre-heater provides little to no benefit, and should not be part of the design. However, the inclusion of an air pre-heater allows for an additional bypass loop. Bypassing the air pre-heater serves to cool the cathode inlet air stream, requiring additional recirculation to pre-heat the air. This boosts the air flow rate, providing more cooling to the fuel cell stack when necessary. Even a well designed system will require additional cooling under instances of increased ambient temperature, decreased ambient pressure, and some fuel perturbations. In addition, including a heat exchanger and bypass valve allows independent control of inlet temperature and flow rate, which is often required for control purposes.

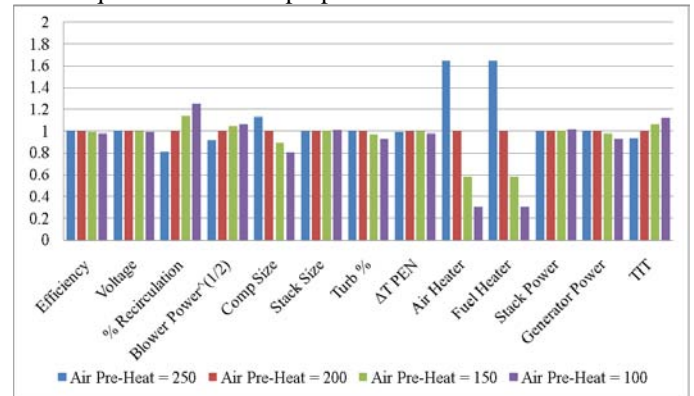


**Figure 8. Design Impact of Air Pre-Heating**

### 5. System Pressure

Table 3 and the Figure 8 show air pre-heat positively affects system efficiency, if only minimally. Air pre-heat can be achieved through heat exchange with fuel cell off gas, or by additional compression. This provides motivation for operating a hybrid system at pressures higher than 5atm. Raising system pressure from 5atm to 10atm yields significant improvement in fuel to electricity performance; from 65% to 69% LHV. Operating at 8atm rather than 5atm raises efficiency to 68% and may be more feasible in the near term than 10atm. Voltage gains and reduced blower power requirements shown in Figure 9 are largely responsible for these improvements.

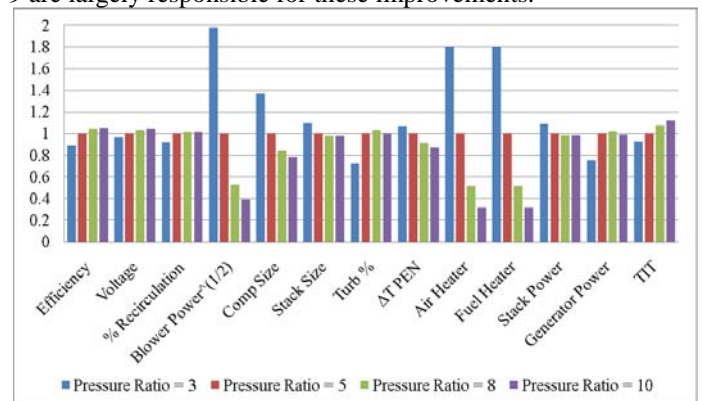


**Figure 9. Design Impact of System Pressure**

## 6. Turbine Efficiency

A key factor in integrating a fuel cell and gas turbine is proper sizing of the two major components. The previous analyses showed fuel cell operating voltage and efficiency produced large variations in optimal compressor size. Efficiency of the turbomachinery also impacts performance and the relative sizing of the components, as shown below. The efficiency shown is the peak efficiency for the characteristic map employed. Most turbines achieve peak efficiencies between 85% and 95%.

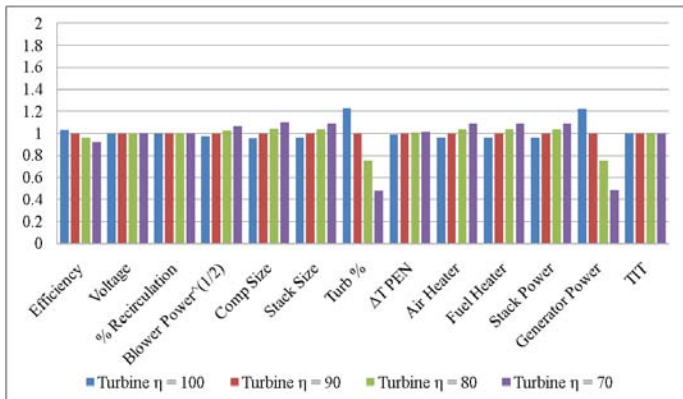


Figure 10. Design Impact of Turbine Efficiency

The turbomachinery only produces 15% of the net power of a hybrid, but Figure 10 demonstrates the large impact of turbine efficiency. A significant portion of turbine power drives the compressor, operating at a fixed load. Thus a 10% reduction in turbine power reduces net power by 25% hybrid power by 4%. Net turbine power diminishes quickly as the turbine operating point shifts away from the high efficiency island of the performance map. This sensitivity highlights the importance of matching the turbine to the fuel cell, since an oversized turbine will operate well below peak efficiency.

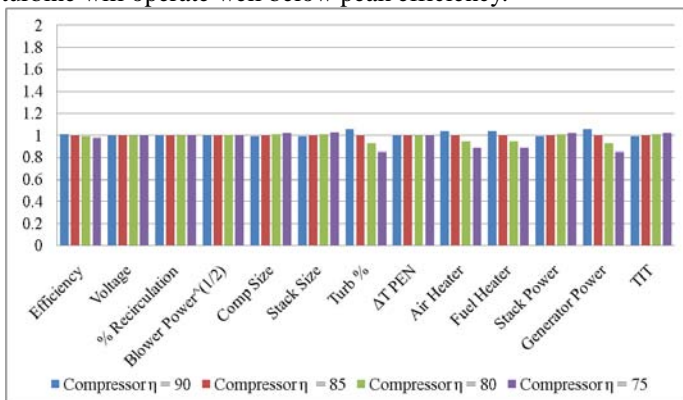


Figure 11 Design Impact of Compressor Efficiency

Compressor efficiency is also highly dependent upon the operating position of the turbomachinery, and thus can compound the impact of an improperly sized system. The effect of diminishing compressor efficiency does not impact system performance as greatly as turbine efficiency; see Figure 11.

Since the air flow passes through at a lower temperature in the compressor, inefficiencies of compression do not produce the same amount of energy loss as in the turbine. However, by looking at the generic axial compressor map one might suppose efficiency drops off quicker when operation moves away from the compressor design point.

## 7. Fuel Cell Operational Temperature

Average fuel cell operating temperature was the final design consideration investigated in this parametric sensitivity study, Figure 12. The overpotential parameters used in this study, particularly ohmic losses, are sensitive to operating temperature. The resulting higher voltage at higher temperatures improves system performance by lowering cooling demands, shrinking the necessary turbomachinery, and thereby increasing the portion of power produced in the fuel cell. Heater size requirements are reduced since heat transfer is more effective at the higher cathode exhaust temperatures. The hotter exhaust and smaller heat exchangers result in an increased TIT, thereby improving the turbomachinery efficiency as well. The impact of fuel cell operational temperature primarily impacts the area specific resistance of a fuel cell. A balance between lower temperatures with higher resistance and higher temperatures with faster degradation determines the operational set point for the fuel cell.

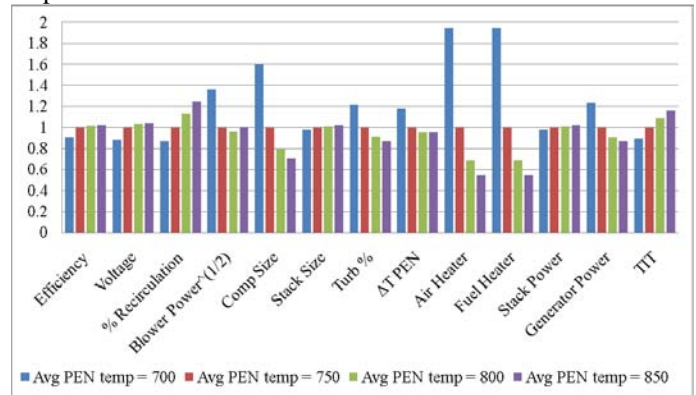


Figure 12 Design Impact of Average Cell Temperature

## OBSERVED TRENDS

Choosing a design point for a FC-GT hybrid represents a difficult trade-off between cost and performance. Additionally, individual components may have different performance characteristics when integrated into such a coupled device. Figure 13 presents the performance impact each independently changed variable has on system performance. Each colored arrow represents variation of a single parameter, as above, and plotted against the respective trends in voltage and efficiency. Figure 13 shows some variables, such as power density and average PEN temperature affect both voltage and efficiency. This is seen to be true of any parameter that significantly affects the fuel cell. Most changes show a positive correlation between voltage and efficiency, as the FC losses are reduced at higher voltages. Variations of fuel

utilizations, however, show a very different trend, as lower voltages correspond to higher efficiency. Turbomachinery efficiencies, compressor and turbine, have little to no effect on voltage, but a small effect on system efficiency. This plot also shows turbine efficiency has a greater impact on performance than compressor efficiency. This is due to the fact that the power production in the turbine is much greater than consumption in the compressor, and thus 10% losses in the turbine account for a greater energy loss than 10% losses in the compressor.

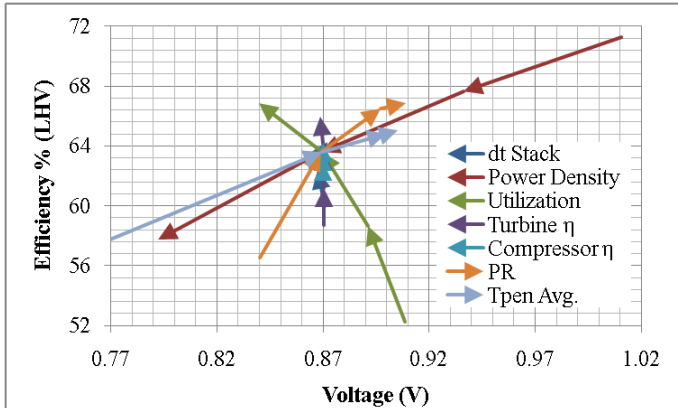


Figure 13 Voltage & Efficiency as Dependent Variables

Figure 14 presents the impact each design consideration has on the amount of cathode recirculation and the portion of total power provided by the gas turbine. These dependent variables closely correlate to the size requirements of the blower and turbine. Arrows indicate an increasing value of the independently varied system parameter. Combining the effects of changing several system parameters may be used to achieve optimum configurations for cost, efficiency, or other parameters of interest. There is significant coupling of the independent variables, thus these arrows cannot simply be added head to tail to define a new system point. The trends of each curve are valid throughout all range of specifiable conditions.

Interestingly the independent variables appear to primarily impact either recirculation or turbine percent power, with the exception of FC operating temperature which impacts both. Turbine efficiency increases the power output of the turbine for the same energy in, thereby increasing turbine power with little effect on the remaining system. The same is true for the compressor efficiency, though it shows a smaller overall impact.

Recirculation primarily controls the air flow rate into the stack, an efficient means of controlling the temperature rise, thus a change in stack temperature rise requires only a change in blower size without affecting the turbine size and power much. Higher recirculation tends to decrease FC performance, generating additional heat per unit of electrical output. This in turn increases the available energy to the turbine and explains the small trend toward higher portions of turbine power at higher recirculation.

Any system parameter that acts to make the FC less efficient typically increase the contribution of power from the turbine by increase the heat losses and energy available to the turbine. Examples of this include power density, utilization and average operating temperature. Higher pressure ratios allow a greater amount of energy to be extracted by the turbine, increasing power, but also increasing cell performance, decreasing losses and the heat available to the turbine. This explains the dramatic difference in arrow length above and below the design point for pressure ratio.

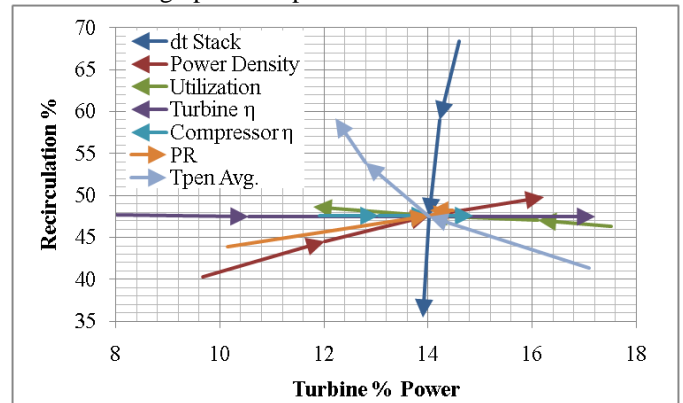


Figure 14 Recirculation and Turbine % Power as Dependant Variables

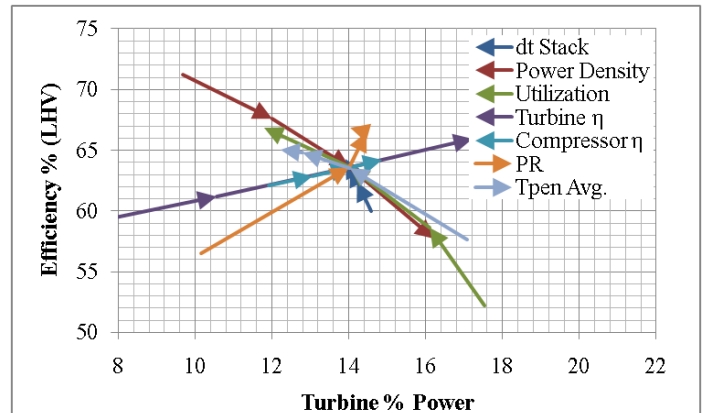


Figure 15 System Efficiency and Turbine % Power as Dependant Variables

Optimally sizing the turbomachinery for the hybrid application is extremely important, but the relationship between turbine size and fuel cell size is complicated. For variables affecting the stack operating efficiency a clear correlation exists between turbine size and system efficiency. Only the data for compressor/turbine efficiency and PR, all relating to turbomachinery performance, do not correspond to what is a clear inverse relationship in Figure 15 combines data from each of the seven parametric studies showing a loss of efficiency for designs where the turbomachinery provides more of the power. This does not mean that using a smaller compressor will make a hybrid system perform better; often this would cause the hybrid to fail completely. What this trend

implies is that designing a system to require a smaller compressor means that you have improved efficiency. The system design point determines the optimal size of the turbomachinery.

## CONCLUSIONS

The primary considerations when designing a hybrid FC-GT system for maximum efficiency are voltage, system pressure, fuel utilization, and PEN operating temperature. The most important selection is the fuel cell operating voltage. The voltage determines power density, with high voltage and relatively low power density giving the best system efficiency. This high efficiency requires a larger stack to produce the same power. Higher system pressure improves voltage and efficiency, but requires sturdier components and axial flow geometry turbomachinery. Radial compressors tend to be limited to pressure ratios of about 5 atmospheres. Most axial turbines are designed for very high pressure ratios, thus an increase in system pressure would bring the design closer to the realm of existing hardware. Higher fuel utilization actually has a negative impact on fuel cell voltage for the configurations considered here, but improves system performance by employing more fuel in the electrochemical reactions. Higher PEN temperature reduces Ohmic resistance, raises TIT and system efficiency, but speeds degradation and possibly requires exotic interconnect and seal materials. The tradeoffs are abundant when selecting a design point, but fuel to electricity efficiencies above 70% (LHV) can be achieved for most designs considered.

An optimal system may achieve ultra-high fuel to electricity conversion efficiency but fall short of economic viability. The fuel cell stack represents the single largest capital cost so that minimizing the stack size requirement reduces cost significantly. Achieving size reductions primarily occurs by raising power density. In the current study, increasing power density from 400 to 500mW/cm<sup>2</sup> reduces the stack size by 25%, with only a 2.6% efficiency penalty. Eliminating the air pre-heating heat exchanger reduces the cost significantly but may diminish the ability to sufficiently control stack operating temperature. Replacing air pre-heat with increased system pressure boosts efficiency if the fuel cell can safely handle the pressure without cracking. Increased pressure improves power density allowing for additional trade-off between efficiency and reducing stack size even further. Optimizing the system with cost minded design choices can produce a relatively power dense system that achieves fuel to electricity conversion rates of 65% (LHV) or better.

## ACKNOWLEDGMENTS

The authors thank the U.S. Department of Defense Fuel Cell Program and Mr. Frank Holcomb of the Construction Engineering Research Laboratory of the Engineer Research and Development Center for partial support of the current work under Contract Number W9132T-08-C-0003.

## REFERENCES

- [1] Brouwer, J., Jabbari, F., Leal, E. M., & Orr, T. (2005). Analysis of a molten carbonate fuel cell: Numerical modeling and experimental validation. *Journal of Power Sources*, 158, 213-224.
- [2] Ferrari, M., Liese, E., Tucker, D., Lawson, L., Traverso, A., & Massardo, A. F. (2007, October). Transient Modeling of the NETL Hybrid Fuel Cell/Gas Turbine Facility and Experimental Validation. *Transactions of the ASME*, 129, pp. 1012-1019.
- [3] Mueller, F., Brouwer, J., Jabbari, F., & Samuelsen, S. (2006, May). Dynamic Simulation of an integrated Solid Oxide Fuel Cell System Including Current-Based Fuel Flow Control. (S. C. Singhal, Ed.) *Transactions of the ASME*, 3, pp. 144-153.
- [4] Xu, J., & Froment, G. F. (1989). Methane Steam Reforming, Methanation and Water-Gas Shift: I. Intrinsic Kinetics. *AIChE Journal*, 35 (1), 88-96.
- [5] Yi, Y., Rao, A. D., Brouwer, J., & Samuelsen, S. G. (2004). Analysis and optimization of a solid oxid fuel cell and intercooled gas turbine (SOFC-ICGT) hybrid cycle. *Journal of Power Sources*, 1-9.
- [6] Roberts, R., Brouwer, J., Liese, E., & Gemmen, R. S. (2004). Dynamic simulation of carbonate fuel cell-gas turbine hybrid systems. *Proceedings of ASME Turbo Expo 2004* (pp. 1-9). Vienna, Austria: ASME.
- [7] Roberts, R., Brouwer, J., Liese, E., & Gemmen, R. S. (2005). Development of controls for dynamic operation of carbonate fuel cell-gas turbine-hybrid systems. *Proceedings of ASME Turbo Expo 2005* (pp. 1-7). Reno-Tahoe: ASME.
- [8] Roberts, R., Brouwer, J., Liese, E., & Gemmen, R. S. (2005). Dynamic Simulation of Carbonate Fuel Cell-Gas Turbine Hybrid Systems. *Journal of Engineering for Gas Turbines and Power*, 127, 1-8.
- [9] Rashidi, R., Berg, P., & Dincer, I. (2009). Performance investigation of a combined MCFC system. *Journal of Hydrogen Energy*, 1-11.
- [10] Burbank, W., Witmer, D., & Holcomb, F. (2008). Model of a Novel Pressurized SOFC-GT Hybrid Engine. *Journal of Power Sources*.
- [11] Milewski, J., Miller, A., & Salacinski, J. (2006). Off-design analysis of SOFC hybrid system. *International Journal of Hydrogen Energy*, 32, 687-698.
- [12] Roberts, R. A., & Brouwer, J. (2006). Dynamic Simulation of a Pressurized 220 kW Solid Oxide Fuel-Cell-Gas-Turbine Hybrid System: Modeled Performance Compared to Measured Results. (S. C. Singhal, Ed.) *Journal of Fuel Cell Science and Technology*, 3, 1-7.
- [13] Pratt, J. W., Brouwer, J., & Freeh, J. E. (2004). Development of a Solid-Oxide Fuel Cell/Gas Turbine Hybrid System Model for Aerospace Applications. *Proceedings of ASME Turbo Expo 2004*, (pp. 1-9). Vienna.
- [14] Wachter, C., Lunderstadt, R., & Joos, F. (2006). Dynamic Model of a Pressurized SOFC/Gas Turbine Hybrid Power Plant for the Development of Control Concepts. *Journal of Fuel Cell Science and Technology*, 3, 271-279.

[15] McLarty, D., & Brouwer, j. S. (2010). novel dynamic quasi-3-dimensional high temperature fuel cell model with internal manifolding. *ASME Fuel Cell 2010*. New York City.

[16] Lunghi, P., Bove, R., & Desideri, U. (2003). Analysis and optimization of hybrid MCFC gas turbines plants. *Journal of Power Sources* , 118, 109-117.

[17] Marra, D., & Bosio, B. (2007). Process analysis of 1 MW MCFC plant. *International Journal of Hydrogen Engineering* , 32, 809-818.

[18] Greppi, P., Bosio, B., & Arato, E. (2008). A steady-state simulation tool for MCFC systems suitable for on-line applications. *International Journal of Hydrogen Energy* , 33, 6327-6338.